

# FEA BASED OPTIMIZATION OF BLANK HOLDER FORCE AND PRESSURE FOR HYDROMECHANICAL DEEP DRAWING OF PARABOLIC CUP USING 2-D INTERVAL HALVING AND RSM METHODS

Thanasan Intarakumthornchai<sup>1</sup>, Suwat Jirathearanat<sup>2</sup>,  
Sirichan Thongprasert<sup>1\*</sup> and Pramote Dechaumphai<sup>3</sup>

<sup>1</sup> Department of Industrial Engineering, Faculty of Engineering,  
Chulalongkorn University, Bangkok, Thailand. 10330

<sup>2</sup> National Metal and Materials Technology Center,  
Phatumtani, Thailand 12120

<sup>3</sup> Department of Mechanical Engineering, Faculty of Engineering,  
Chulalongkorn University, Bangkok, Thailand. 10330

E-mail : intara99@yahoo.com<sup>1</sup>, suwatj@mtec.or.th<sup>2</sup>, sirichan.t@chula.ac.th<sup>1\*</sup>  
and fmepdc@eng.chula.ac.th<sup>3</sup>

## ABSTRACT

2-D interval halving and response surface methods are presented to determine optimal process parameters of linear pressure and constant blank holder force profiles for hydromechanical deep drawing of a parabolic cup using finite element analysis. The optimization goal is to obtain the process parameters that minimize part thinning without any cracks and wrinkles. Part thinning and geometry-based wrinkle constraint functions are employed to quantify cracking and wrinkling severity. A response surface of part minimum thickness as a function of maximum internal pressure and blank holder force is constructed by using the data collected during the 2-D interval halving method. The optimum process parameters are then determined from the obtained surface. It is found that the method is capable to determine the optimal blank holder force and linear pressure profiles for hydromechanical deep drawing of the parabolic cup.

## KEYWORDS

2-D interval halving method, response surface method, hydromechanical deep drawing, finite element analysis.

# I. Introduction

Parabolic shaped cups are commonly used in spot lights and car headlamps as light reflectors. Due to their particularly pointy and tapered shape, if poorly designed, the cupping process can easily form part with wrinkles or fractures. These parabolic cups often require at least six forming steps using conventional deep drawing process to produce good cups. The hydromechanical deep drawing (HMD), a relatively new forming process where solid die cavity is replaced by highly-pressurized water, can potentially form these cups successfully by using just a single step with improved part dimensional accuracy [1].

When applying hydromechanical deep drawing, key process parameters affecting part quality are blank holder force and counter pressure. Excessive blank holder force and counter pressure can lead to fracture. On the other hand, insufficient blank holder force and counter pressure can also lead to wrinkle. Therefore, proper blank holder force and proper counter pressure are very important in carrying out the forming process successfully. This research proposed an FEA based optimization method to optimize these two process parameters.

Zhang et al. [1] - [3] studied effects of anisotropy, pre-bulging, counter pressure and blank holder force on formability of several parts such as round cups, parabolic cups and rectangular boxes in hydromechanical deep drawing process using both finite element analysis simulations and experiments. Lang et al. [4] – [5] investigated forming of a complex square cup and a round cup using the hydromechanical deep drawing process with uniform pressure by both experiments and finite element analysis simulations. They showed that the simulated results reasonably agreed with the experimental results.

Response Surface Methodology is a method for constructing global approximations of valued objective and constraint functions based on functional evaluations at various points in the design space. Many researchers have applied RSM to simulation models in computational mechanics field. Roux et al. [6] discussed experimental design techniques and regression equations for structural optimization. Response surface methodology combining with stochastic finite elements were used by Kleiber et al. [7] for reliability assessment in metal forming. Wang and Lee [8] used response surface methodology and finite element analysis to control strain path during forming process with space-variant blank holder force.

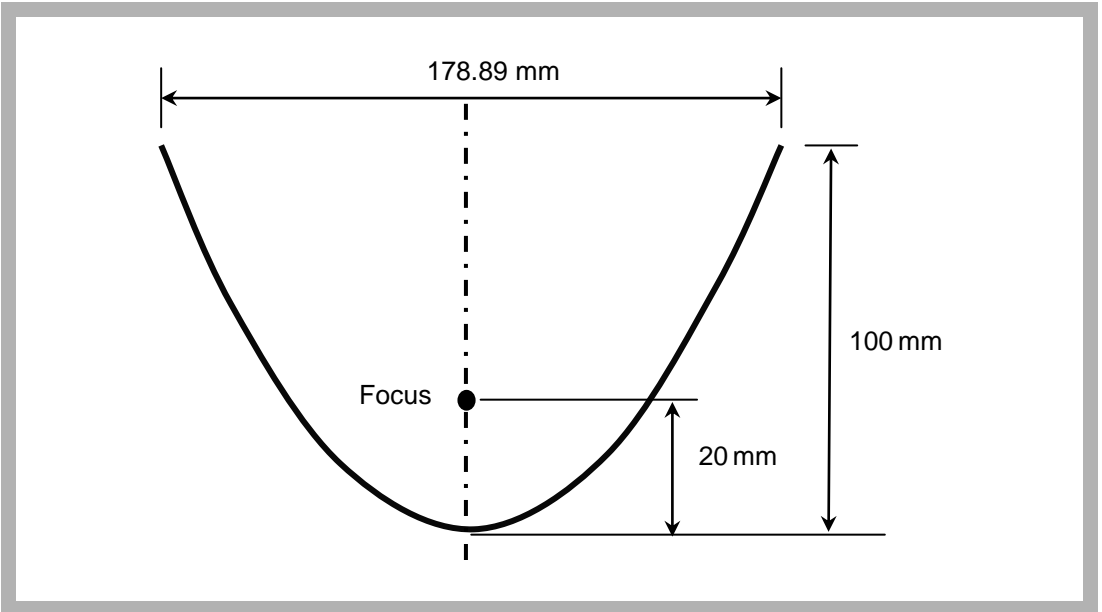
In this research, RSM is applied to determine optimal constant blank holder force and linear pressure from a feasible region. In this work, 2-D interval halving method is combined with response surface methodology to optimize the process parameters for hydromechanical deep drawing of a parabolic cup.

## II. Parabolic cup and Finite element analysis

### 2.1 Parabolic cup

Dimensions of the parabolic cup used in this study are shown in Figure 1. This particular part geometry is prone to fracture and wrinkle during normal stamping process, if the process parameters are not applied properly. Deep drawing of these parabolic parts is difficult because of the fact that the drawing load must be transmitted through only a very small cross section area of the sheet. Thus, the risk of local cracking is high even for small drawing ratios. Moreover, there is a relatively large unsupported area between the die and the punch. Consequently, the circumferential compressive stresses can easily cause side wall wrinkles in the unsupported area of the forming part.

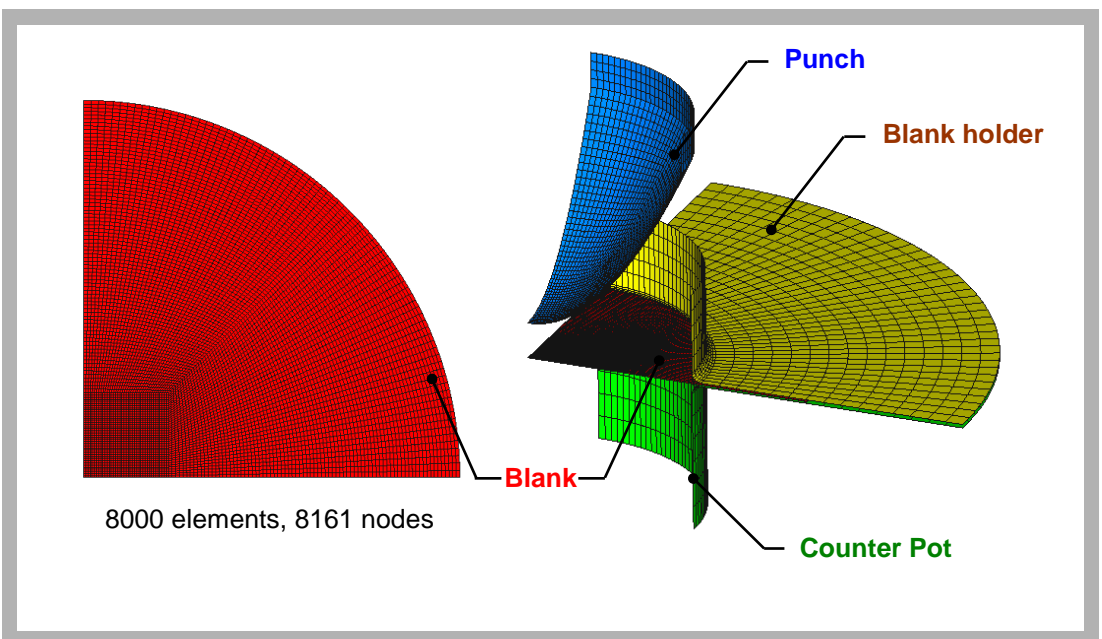
**Figure 1**  
Parabolic cup  
dimensions.



## 2.2 Finite element analysis and hydromechanical deep drawing process

A nonlinear dynamic explicit code, LS-DYNA, is used for the analysis. To take advantage of part symmetry and material property symmetry, i.e. anisotropy, a quarter finite element model, Figure 2, is used as to reduce computational time. The blank is meshed with 8,000 quadrilateral elements and 8,161 nodes. Belytchko-Tsay thin-shell elements are selected in the analysis.

**Figure 2**  
Finite element model  
(a quarter model)



There are many constitutive material models that can be used to model the steel blank. These are Von Mises isotropic material model (material type 18), Barlat-Lian's three-parameter model (material type 36) and Hill's transversely anisotropic model (Hill 1948 model; material type 37). It was shown by Zhang et al. [1] that a good agreement between the simulation and experiment is obtained when using either Hill's transversely anisotropic model or Barlat-Lian's three-parameter model. In this work, Barlat-Lian's three-parameter model is used for the blank material model. Barlat recommends  $M = 8$  for the face centered cubic (FCC) materials,  $M = 6$  for body centered (BCC) materials. AISI 1008 (JIS G 3141 SPCC) sheet steel was found to have BCC structure [9], so  $M = 6$  was applied in this work. Mechanical properties of



Time scaling of 1,000 was used to guarantee a reasonable computational time, i.e. using an artificial punch speed of 5.0 m/s while a typical real punch speed is 5.0 mm/s. In all the simulations of this work, the pre-bulging pressure and corresponding blank holder force are 3 MPa and 25,000 N, respectively. The pre-bulging stage takes place for a dome height of 20 mm with a maximum plastic strain of 2-8%.

### III. Defect criteria

In hydromechanical deep drawing process of a parabolic cup, the blank is initially bulged, and becomes in contact with punch. As the punch is descending downwards, both pressure and blank holder force keep the blank stretching for successfully forming as depicted in Figure 4. The main part defects are cracks and wrinkles. The thinnest area often occurs in the area contacted with punch head, while severe side wall wrinkling is taken place in the unsupported area and flange wrinkling happens in the flange area.

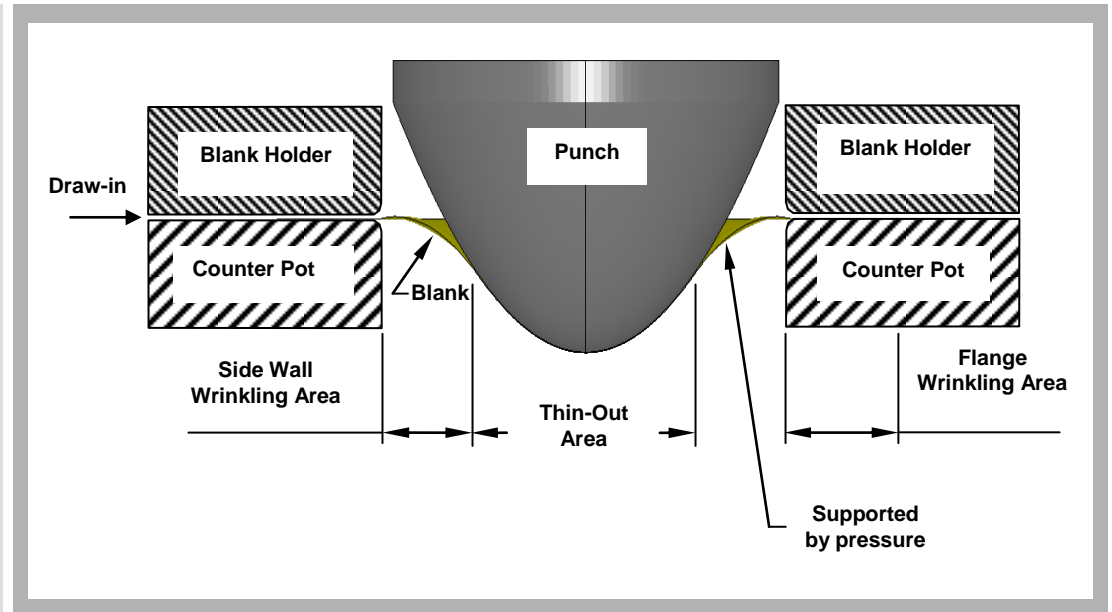


**Figure 4**  
The schematic of the HMD process of parabolic cup

#### 3.1 Crack criterion

Generally, fracture can be predicted by: (1) strain based criteria, e.g. forming limit diagrams (FLDs) [11] and maximum part thinning [12]; (2) stress based criteria, e.g. forming limit stress diagrams (FLSDs) [13]; and (3) ductile damage criteria, e.g. the Cockcroft and Latham criterion [14]. Part wall thinning is commonly used in industry to indicate probability of fracture [15]. Therefore, in this present study, the maximum wall thinning was selected as a fracture criterion. However, this is an approximate criterion because the critical maximum thinning is known to be affected by strain paths. From conducting several hydromechanical deep drawing simulations of AISI 1008 parabolic parts, the parts cracked at minimum major and minor strains around 0.39 and 0.09, respectively. This strain condition is located just above the FLC (derived from M-K model [16]) on right hand side, which corresponds to part thinning of 39%. The location of crack site is in the punch nose area and it is found to be in the same location as the part thinnest area as well, 39% as shown in Figure 5. For the AISI 1008 parabolic part, therefore, the thinning criterion limit ( $Thin_{Lim}$ ) was chosen to be 39% as it corresponds with the part fracture predicted by the forming limit curve.

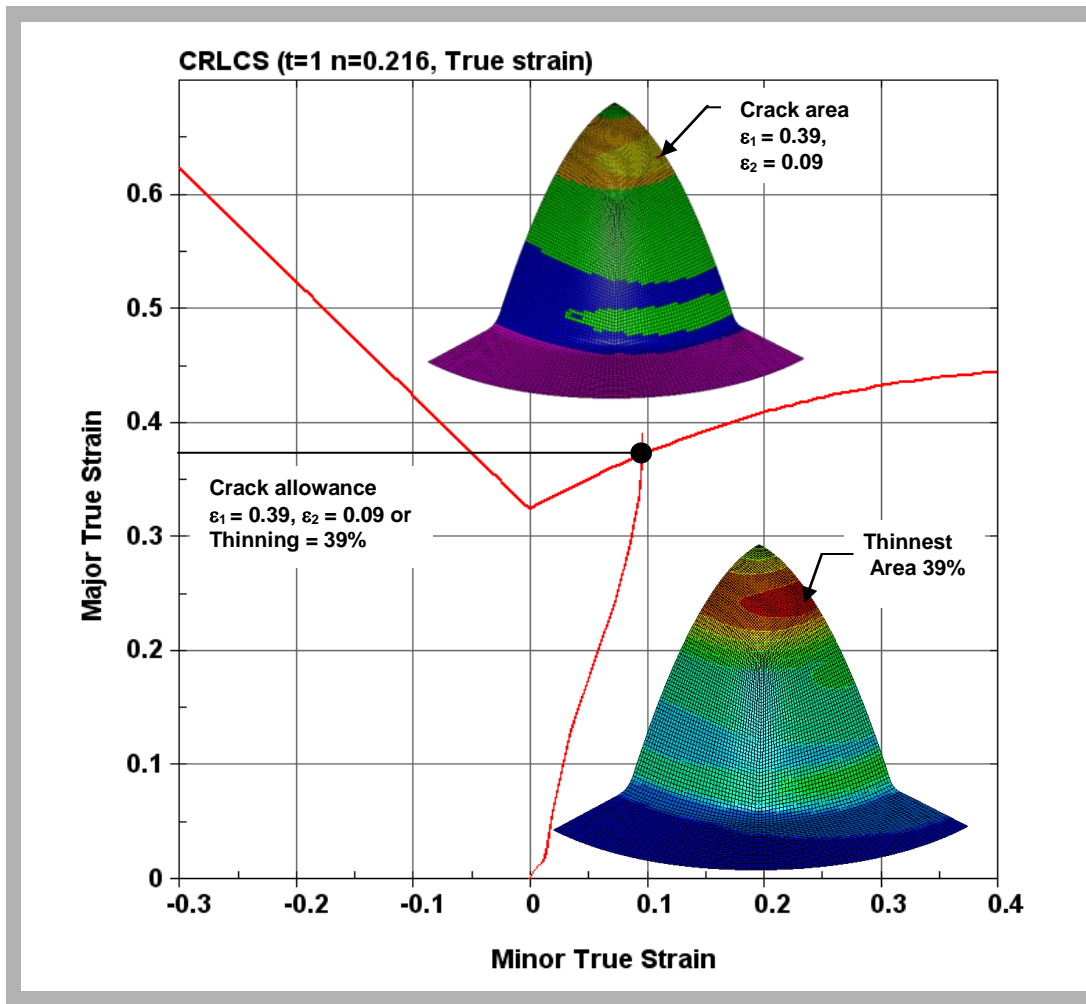


**Figure 5**  
 Comparison between formability and thinning in AISI 1008 parabolic cup of HMD process with crack criteria

## 3.2 Wrinkle criterion

Two types of wrinkle can occur in the parabolic parts: a) flange wrinkle and b) sidewall wrinkle. In finite element simulation, both wrinkle types can be indicated by certain geometry based rules or stress based rules. Owing to its simplicity, a geometry based method was used to indicate and quantify the wrinkles in this work.

### 3.2.1 Sidewall wrinkle

Due to circumferential compressive stresses in the flange area, the blank tends to buckle and develops flange wrinkles. The flange wrinkle amplitude (FAM) can be inferred from the gap distance between blank holder surface and counter pot addendum surface as shown in Figure 6 [15]. To determine the critical FAM value, several forming simulations were conducted with various fixed gap distance. The gaps were varied from 1.00, 1.01, 1.02, 1.03, 1.04, 1.05, 1.06, 1.07 and 1.08 mm respectively. The results are shown in Figure 7. The flange wrinkle can be easily visualized on the parts if FAM is over 1.05, which agrees with Sheng et al. [15]. They used 5% of nominal sheet thickness to be flange wrinkle criteria in their study. This critical wrinkle amplitude, however, would be different for different parts depending on part functionality. In this parabolic part with HMD process, the flange wrinkle limit ( $FAM_{Lim}$ ) was chosen as 1.05 mm.

**Figure 6**  
Measurement of flange wrinkling amplitude (FAM)

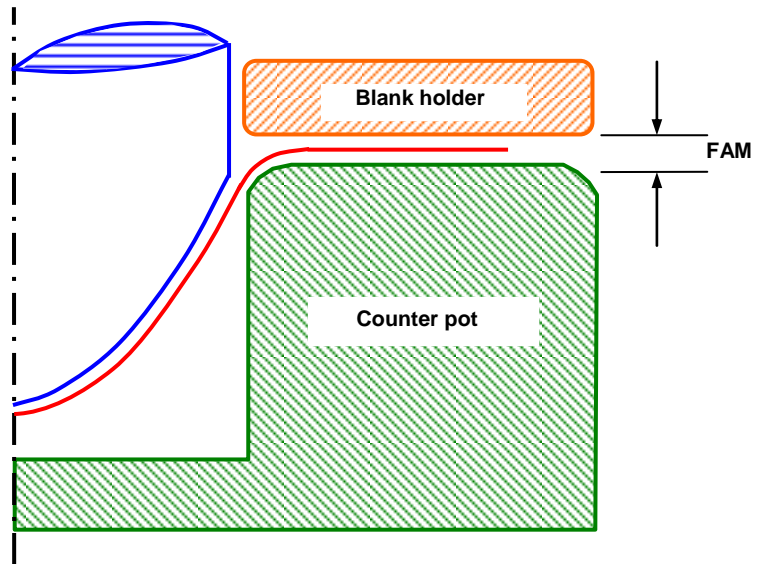
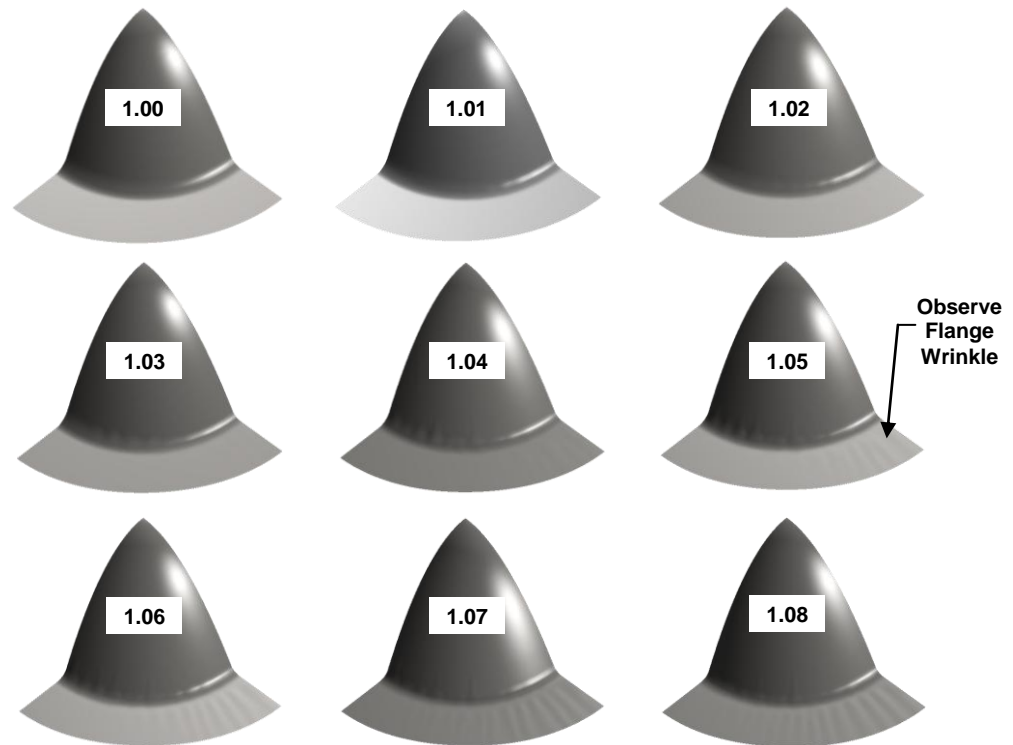


**Figure 7**  
Flange wrinkling amplitude (FAM) results by varying gap



### 3.2.2 Wrinkle criterion

The parabolic shape makes this part family very susceptible to sidewall wrinkle formation. During hydromechanical drawing of this part, large hydraulic pressures are needed to suppress these potential sidewall wrinkles. The severity of these wrinkles can be quantified by normal distances from part wrinkle-affected nodes to the corresponding punch surfaces, which are referred to as the sidewall wrinkle parameter (SW) as shown in Figure 8. The part is found to be defective when SW becomes larger than 5% of the initial part thickness, which is referred to as sidewall limit ( $SW_{Lim}$ ). From the middle surface simulation model, the  $SW_{Lim}$  value in this study is 0.525.

Upon completion of a forming simulation, normal distances between the punch and formed part mesh are measured at every node as shown in Figure 9. The longest distance is chosen to be the SW.

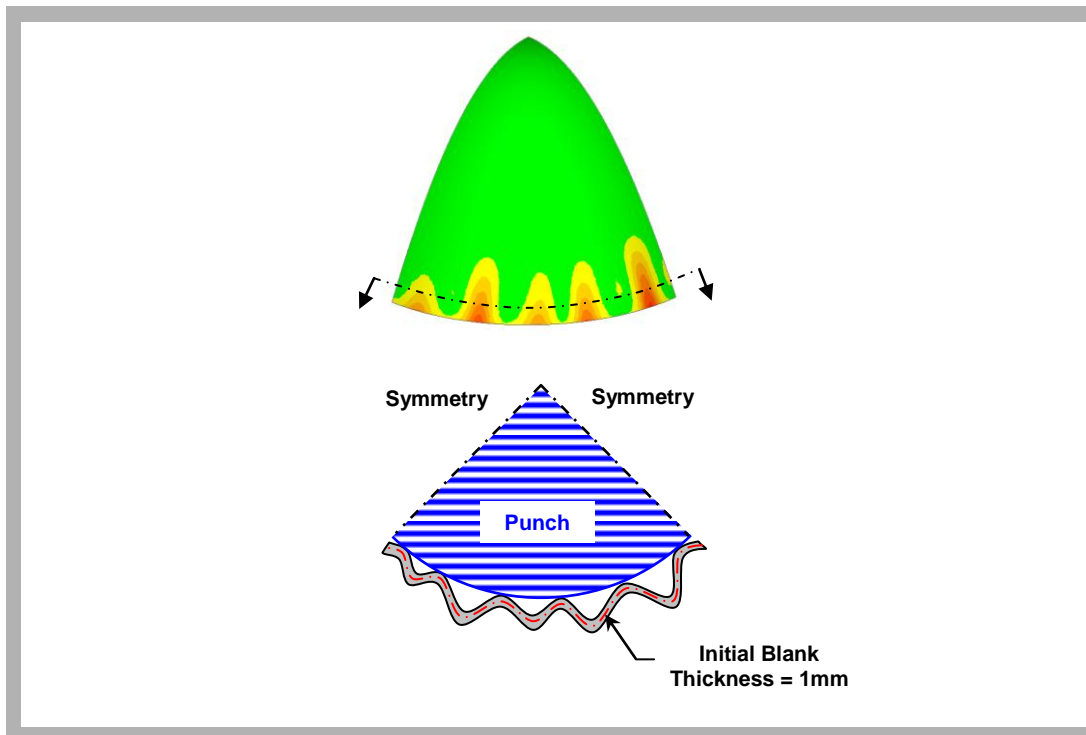


**Figure 8**  
Sidewall wrinkles

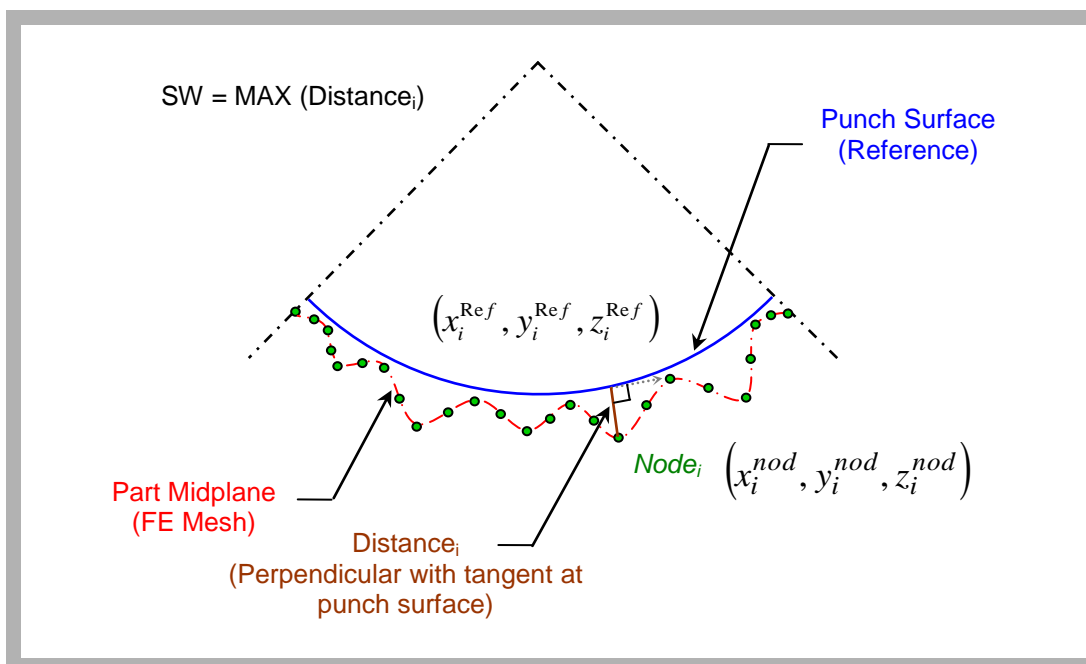


**Figure 9**  
Measurement of  
sidewall wrinkle  
(SW)

## IV. Search Method

In this section, a procedure to determine a feasible region is described. Analytical equations are first used to determine search space bounds. Then, a feasible region is obtained through 2-D interval halving. A flowchart describing the optimization procedure of process parameters is given in Figure 10.

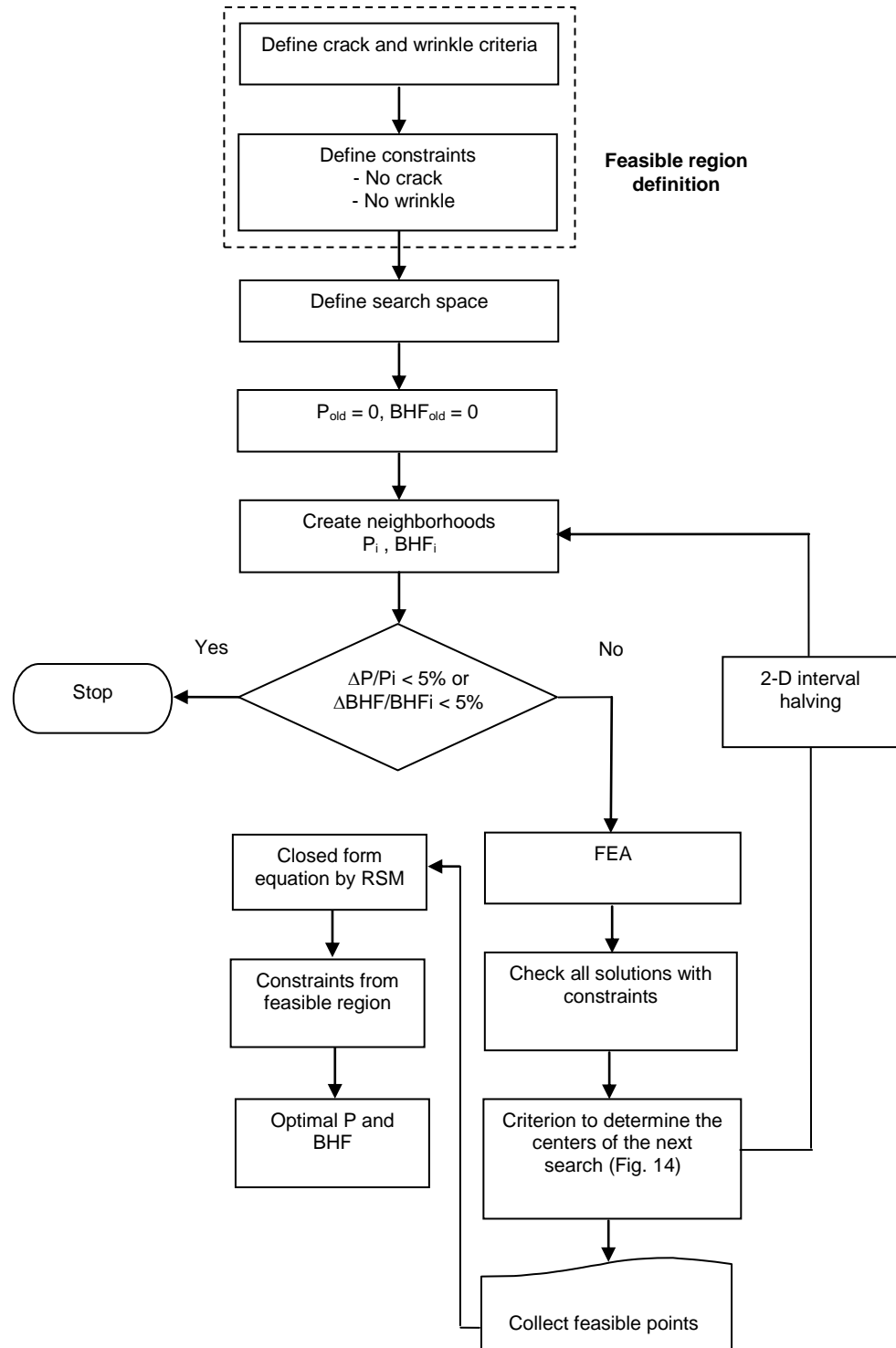


**Figure 10**  
Flow chart to determine  
the optimal P and BHF

#### 4.1 Search space bounds and process window

The minimum pressure  $p_{\min}$  is the smallest pressure that will initiate sheet deformation and can be estimated by Eq.1. The maximum pressure  $p_{\max}$  is the largest pressure beyond which the sheet will burst. Eq.2 determines this maximum pressure [17], see Figure 11.

$$p_{\min} = \frac{\sigma_{\text{yield}} \times t}{r_{\min}} \quad (1)$$

where  $\sigma_{yield}$  = the yield strength of the blank material (MPa),  $t$  = the wall thickness of the blank (mm) and  $r_{min}$  = the minimum radius of the part (mm).

$$p_{max} = \frac{\sigma_{UTS} \times t}{r_{min}} \quad (2)$$

where  $p_{max}$  = maximum pressure to begin forming (MPa),  $\sigma_{UTS}$  = the ultimate strength of the blank material (MPa).

The minimum BHF can be estimated using Eq. 3, which follows the idea that the BHF should be at least large enough to suppress the flange wrinkle throughout the process.

$$MinF_{BH} = p_n \frac{\pi}{4} (D_0^2 - D_s^2) + F_{BH/pressure} + F_{BH/bulge} \quad (3)$$

where  $p_n$  = the blank holder pressure,  $D_0$  = outgoing blank diameter,  $D_s$  = sealing diameter,  $F_{BH/pressure}$  = the vertical force from pressure acting on the blank holder and  $F_{BH/bulge}$  = the bulge force acting on the blank holder.

The blank holder pressure  $p_n$ , which is the normal pressure between the sheet and the blank holder and between the sheet and the draw ring for axisymmetric components, one finds in Eq. 4

$$p_n = 0.002 \dots 0.0025 \left[ (\beta_0 - 1)^3 + 0.5 \frac{D_{punch}}{100t_0} \right] \sigma_{UTS} \quad (4)$$

where  $\beta_0 = \frac{D_0}{D_{punch}}$ ,  $D_{punch}$  = punch diameter,  $t_0$  = outgoing blank thickness,  $\sigma_{UTS}$  = ultimate tensile strength,  $\sigma_{yield}$  = yield tensile strength.

$F_{BH/pressure}$  is the vertical force acting on the blank holder in the gap between the draw ring and sheet metal. It can determine in Eq. 5.

$$F_{BH/pressure} = \frac{\pi}{4} p_c (D_s^2 - D_{BH}^2) \quad (5)$$

where  $p_c$  = working pressure,  $D_{BH}$  = inner blank holder diameter.

$F_{BH/bulge}$  is the bulge force acting on the blank holder in the area between the inner diameter of the blank holder and the contact line. It can compute in Eq. 6.

$$F_{BH/bulge} = \sigma D_{BH} \pi t \quad (6)$$

where  $\sigma = \frac{p_c}{4t} (D_{BH} - D_{contact})$  and  $D_{contact}$  = contact line diameter

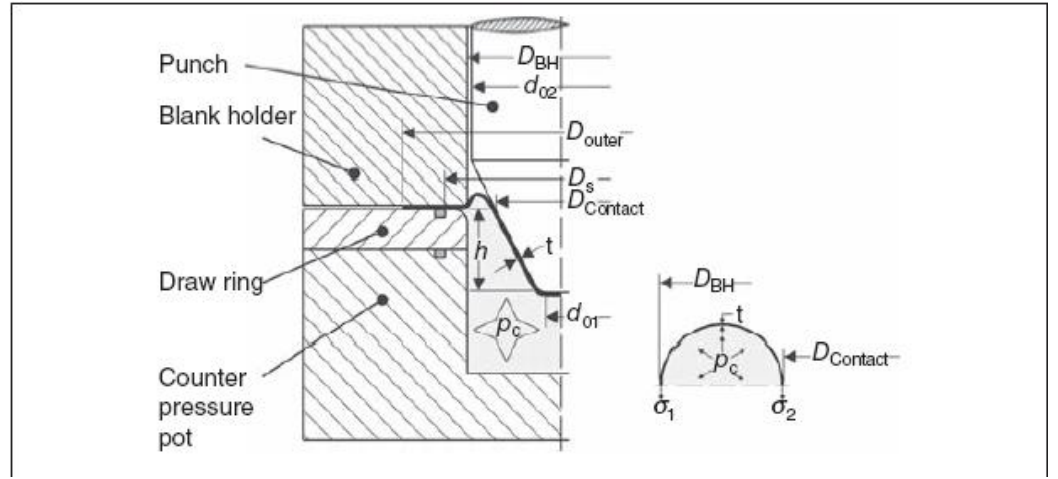
As for the maximum BHF, in this work, it is chosen to be the upper limit of the press capability which is 104 tons (26 tons for the quarter model used in this study).

Finally, the search space bounds are found to be as follows:

$$L_i \leq P \leq U_i; \quad 22.00 \text{ MPa} \leq P \leq 40.00 \text{ MPa}$$

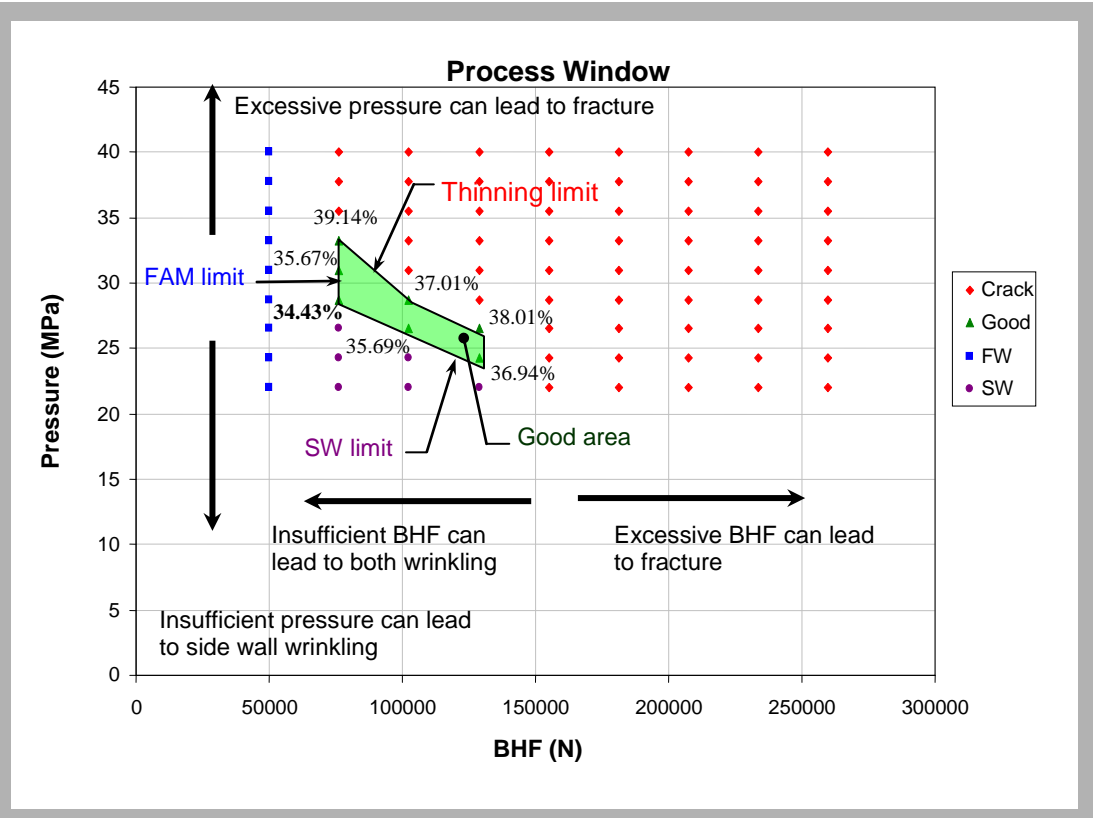
$$L_i \leq \text{BHF} \leq U_i; \quad 50,000 \text{ N} \leq \text{BHF} \leq 260,000 \text{ N}$$

**Figure 11**  
Forming a bulge with hydromechanical deep drawing components with tapered shaped walls [17]



After having established the search bounds, a process window (a diagram showing feasible and defective regions of all forming process conditions) was generated by separating the range of pressure and blank holder force into nine points and conducting FE analyses were conducted to investigate all combinations of BHF and pressure chosen. In this case, the total number of combinations between P and BHF is 81 simulations. A crack was determined by the crack criterion and plotted on to the process window with  $\blacklozenge$  symbol. The flange wrinkle (FW) was determined by the FW criterion and plotted on to the process window with  $\blacksquare$  symbol. The side wrinkle (SW) was determined by SW criterion and plotted on to the process window with  $\bullet$  symbol. All the good part forming conditions were plotted on to process window with  $\blacktriangle$  symbol.

**Figure 12**  
Process window of the parabolic cup



The process window was constructed in a diagram as shown in Figure 12. The left boundary shows a flange wrinkle limit caused by insufficient blank holder force. The right boundary shows a crack limit caused by excessive blank holder force. The upper boundary is another crack limit caused by excessive pressure. The lower boundary is a sidewall wrinkle limit affected by insufficient pressure. The region bounded by all the

defective limits mentioned is the successful forming area so called "feasible region". For this part, there are three ways to enter the feasible region; 1) from crack boundary, 2) from flange wrinkle boundary and 3) from side wall wrinkle boundary. Solutions accessed from the crack boundary will have thinning near the thin limit (39%). The solutions accessed from the flange wrinkle boundary will have FAM near the FAM limit (1.05). The solutions accessed from the side wall wrinkle boundary will have SW near the SW limit (0.525) and the maximum thinning less than that accessed from the thinning boundary. For example, from the process window, BHF as 76,250 N (for quarter) and pressure as 28.75 MPa would form a part with maximum thinning less than 34.43%, FAM of 1.040 mm (no flange wrinkle), SW of 0.487 mm (no side wall wrinkle).

## 4.2 Search method and neighborhood determination

It is evident from the previous section that a numerous number of simulations has to be conducted to find the feasible region of the parts, thus expensive and time consuming. To reduce a number of simulations in order to find the feasible region of the parabolic cup forming, the 2-D interval halving method was applied.

Neighborhoods were created by separation of the search space into four areas equally as described by Figure 13. The center points of the four areas are evaluated through simulation runs. Center points that are found to form a good part (i.e. acceptable wrinkles and thinning) are labeled as the feasible points.

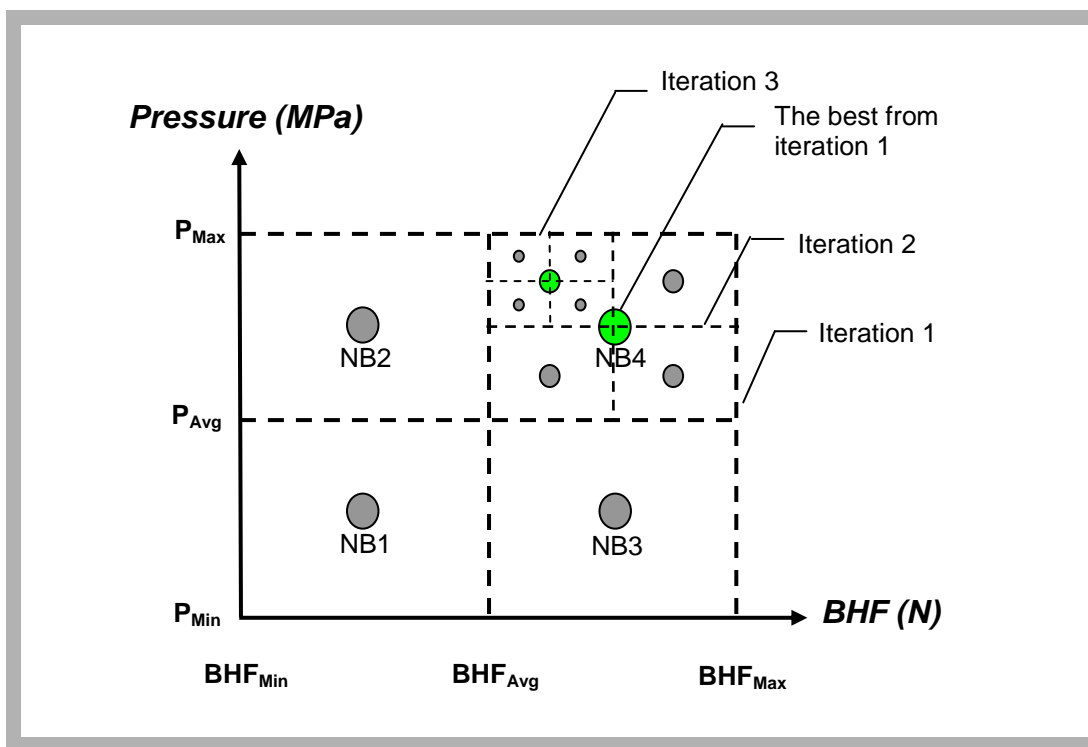


**Figure 13**  
Schematic of 2-D  
interval halving search  
algorithm

In each search iteration, all the center points of the current neighborhoods are evaluated through the finite element analysis simulation. A center point in the process parameter space is said to be a feasible point if it forms a part with the defect parameters; SW, FAM, and % thinning, under their limits;  $SW_{Lim}$ ,  $FAM_{Lim}$  and  $Thin_{Lim}$ , respectively. All the center points in each iteration are also compared to determine the one with the best quality to be the center of next search.

2-D interval halving method was applied as the search method in this study. In each iteration, the method searches for center point(s) in the current neighborhoods that is either of (a) feasible forming parameters or (b) able to be the best quality for the center point. Then, these points determined are to be center points of new neighborhoods, which are split into four regions, to be evaluated in the next iteration. These search iterations keep progressing until the forming parameters (blank holder force and pressure) of newly found points are only 5% different from the previous point. The search objective is to find process conditions with linear pressures and constant blank holder forces able to form a part with *minimum thinning* with *no crack* and *no wrinkles*.

Based on the knowledge obtained from the process window, Fig. 12, search direction should be approaching to the feasible region from the sidewall wrinkle boundary (SW limit line).

The schematic to determine the center of the next search for the minimum thinning is shown in Figure 14. The neighborhoods with cracks are considered firstly by using the thinning criterion as defined in Eq. 7. This is because if all neighborhoods pass the thinning criterion (to have the thin defect as zero or negative), the search will be entering the feasible region from FAM or SW limit, as suggested.

$$Thin \ Defect = \left( \frac{Thin_i - Thin_{Lim}}{Thin_{Lim}} \right) \quad (7)$$

If the neighborhoods pass both the thinning criterion and FAM criterion, as defined in Eq. 8, the search will proceed from the SW limit as a result the parts will tend to have minimum thinning. In case of FAM is the final consideration, the search does not guarantee that the formed parts will have minimum thinning quality due to the fact that thinning values from of parts accessed from the FAM limit vary considerably.

$$FW \ Defect = \left( \frac{FW_i - FW_{Lim}}{FW_{Lim}} \right) \quad (8)$$

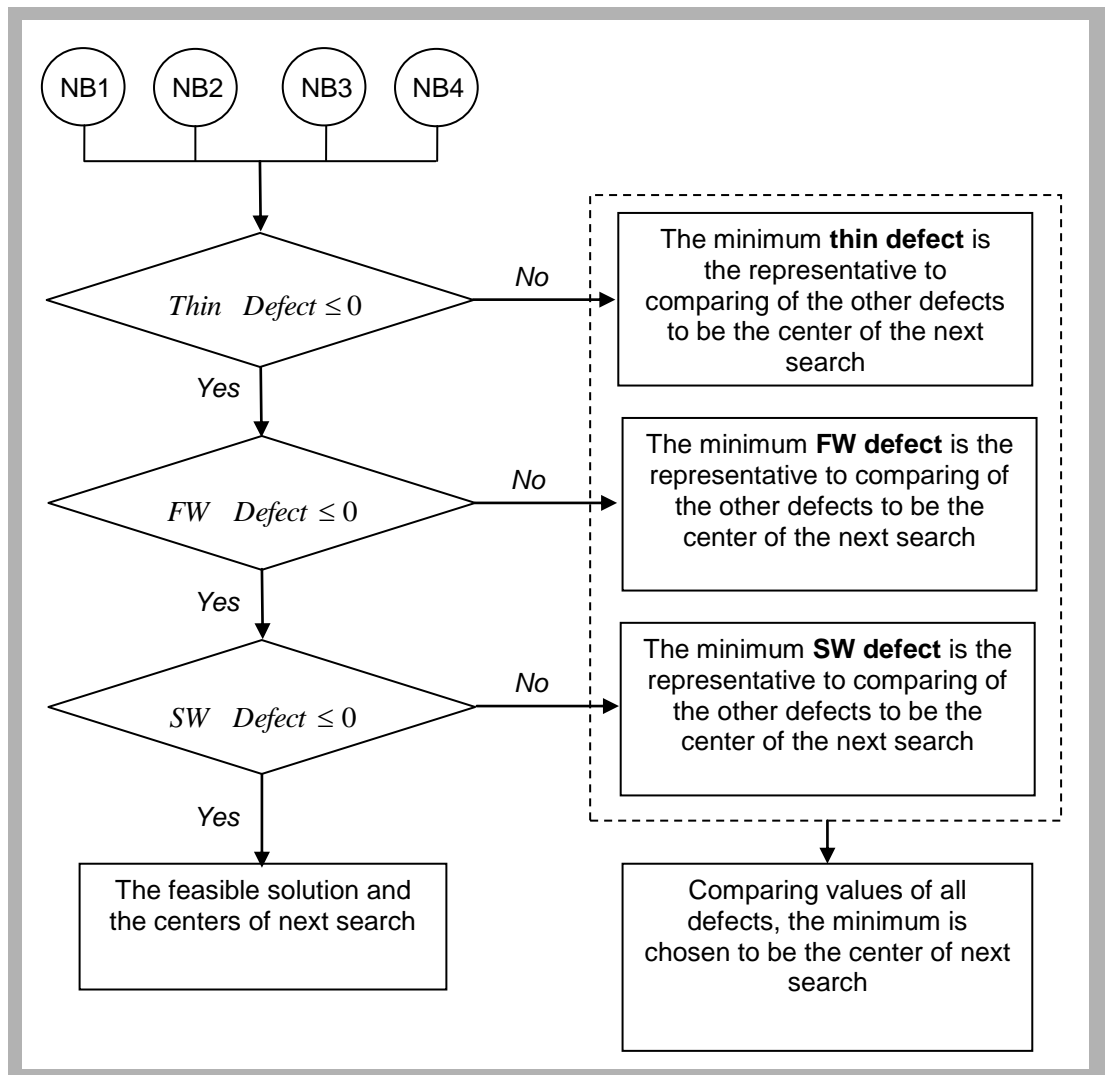


**Figure 14**  
Criteria to determine the centers of the next search procedure

After having passed the cracking assessment and flange wrinkle assessment, the neighborhood can still exhibit sidewall wrinkle. Hence, the SW is the final consideration. If all neighborhoods passed the thinning criterion, FAM criterion and SW criterion (defined in Eq. 9) the parts are obviously feasible. If the neighborhoods do not pass any of the criteria, the valued indexes (Eq. 7 to 9) of all defects are compared.

The part that has minimum defect index is to be the center of the next search because it is nearest the boundary of feasible region.

$$SW_{Defect} = \left( \frac{SW_i - SW_{Lim}}{SW_{Lim}} \right) \quad (9)$$

The 2-D interval halving method was applied as the search method in this study. In each iteration, the method searches for the center point(s) in the current neighborhoods that is either of: (a) feasible forming parameters or (b) able to be the best quality for the center point (passed in Figure 14). Then, these points are to be center points of new neighborhoods, which are split into four regions and evaluated in the next iteration. The search iteration procedure keeps progressing until the forming parameters (pressure and blank holder force) of newly found points are only 5% different from the previous point. In this study, 9 feasible points were determined after 16 neighborhoods (3 iterations) were evaluated.

These feasible points form a bounded feasible region as shown in Figure 15. Then, the optimization goal is only to determine the best process parameters within this feasible region (i.e. BHF and max. pressure) that minimize part thinning.

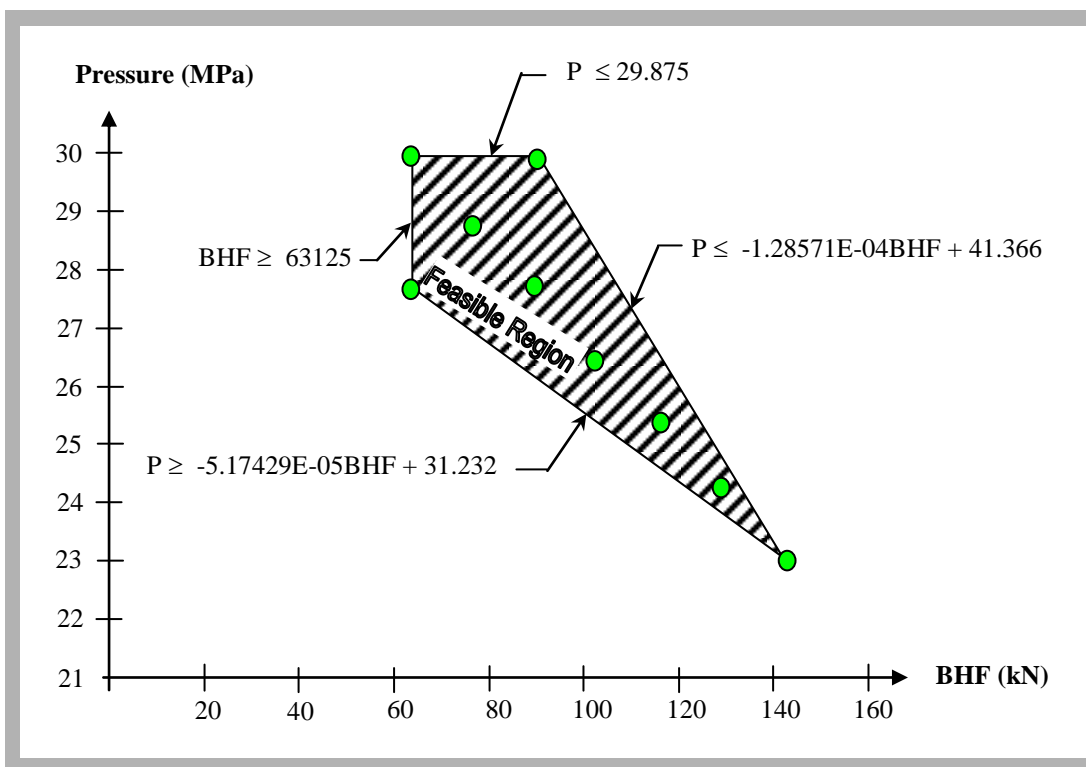


Figure 15  
Feasible region

## V. Response Surface Method (RSM)

Quadratic polynomial form, Eq. 10 [18], of RSM was used to describe the relationship between the process parameters (BHF and maximum pressure) and resultant part maximum thinning percentage in Eq.11. Using the least square polynomial approximation, the response surface over the feasible region, which has been determined through the 2-D interval halving method, is given by Eqs. (12-16).

$$y = \beta_0 + \sum_{j=1}^k \beta_j x_j + \sum_{j=1}^k \beta_{jj} x_j^2 + \sum_{i=1}^{k-1} \sum_{j=i+1}^k \beta_{ij} x_i x_j \quad (10)$$

$$\text{Thinning} = \beta_0 + \beta_1 \text{BHF} + \beta_2 P + \beta_3 \text{BHF} \cdot P + \beta_4 \text{BHF}^2 + \beta_5 P^2 \quad (11)$$

$$\begin{aligned} \text{Thinning} = & 30.6408 - 1.39969 \times 10^{-4} \text{BHF} + 0.0322575 P \\ & + 4.88183 \times 10^{-6} \text{BHF} \cdot P + 5.02062 \times 10^{-10} \text{BHF}^2 \end{aligned} \quad (12)$$

Subjected to:

$$P \leq 29.875 \quad (13)$$

$$BHF \geq 63125 \quad (14)$$

$$P \leq -1.28571E-04BHF + 41.366 \quad (15)$$

$$P \geq -5.17429E-05BHF + 31.232 \quad (16)$$

The feasible values of BHF and pressure from 2-D interval halving method are input in Eq. 12 to compute the thinning to be compared with the finite element simulation results. The errors are shown in table 2. The error percentages were lower than 0.25%; therefore, Eq. 12 can calculate the thinning from BHF and pressure within the constraints from Eq. 13 - 16.

BHF (N)	Pressure (MPa)	%Thinning (FEA)	% Thinning (from Eq. 12)	Error	%Error
102500	26.5	35.69	35.68386	0.006139	0.02%
76250	28.75	34.43	34.51647	-0.08647	-0.25%
128750	24.25	36.94	36.96649	-0.02649	-0.07%
63125	27.625	33.21	33.21004	-4.2E-05	0.00%
63125	29.875	34.02	33.97599	0.044006	0.13%
89375	27.625	35.11	35.08576	0.024238	0.07%
89375	29.875	36.14	36.14005	-4.7E-05	0.00%
141875	23.125	37.65	37.65101	-0.00101	0.00%
115625	25.375	36.35	36.31077	0.039231	0.11%

**Table 2**

The thinning comparison between FEM and thinning equation on Eq.12

The approximated response surface is shown in Figure 16. Simplex method was applied to locate the optimal point, i.e. the lowest point of the surface. The optimal point is BHF of 63,125 N and maximum pressure of 27.625 MPa for the quarter model, resulting in part maximum thinning of 33.21%. In the same condition the finite element method conducts the maximum thinning as 33.21% that is the same value from Eq. 12 and gives FAM as 1.046 mm (no flange wrinkle), SW as 0.489 (no side wall wrinkle). The solutions were shown in Figure 17.

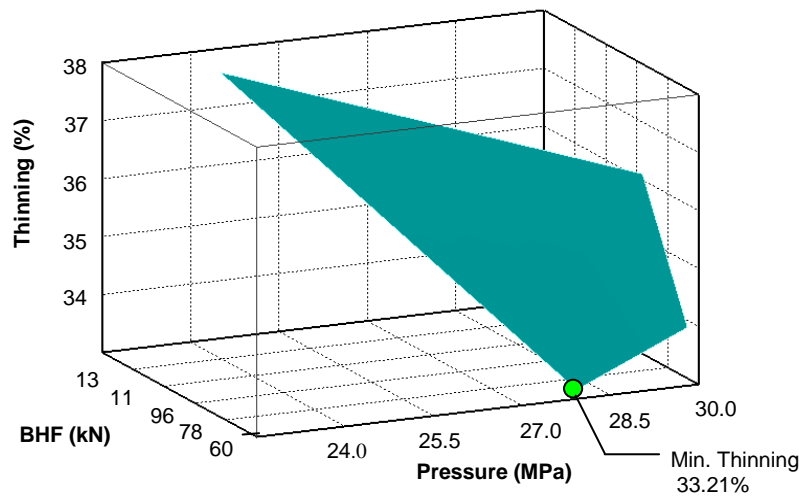


**Figure 16**  
Part thinning response surface of two variables; BHF and P with constraints

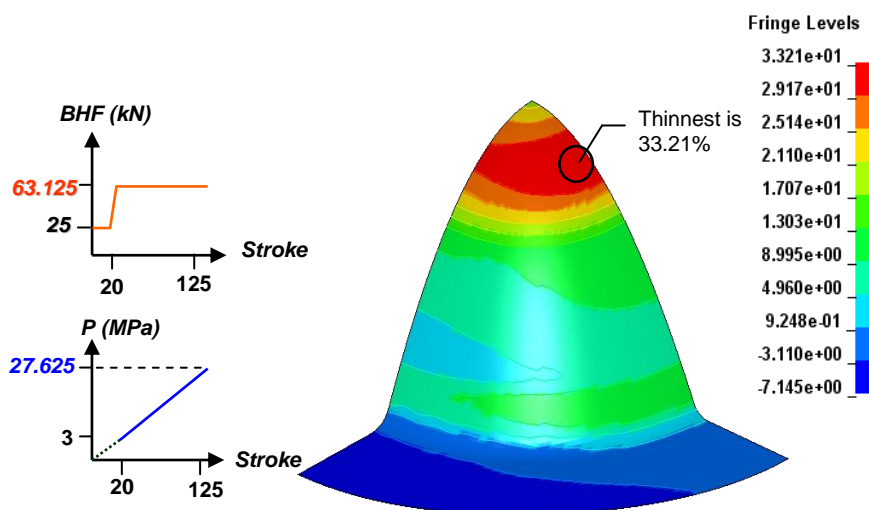


**Figure 17**  
Part thickness distribution formed by the optimized BHF and P from RSM

## VI. Conclusions

The response surface method coupled with the 2-D interval halving method was applied to optimize the necessary process parameters of the constant blank holder force and linear pressure profiles for the hydromechanical deep drawing (HMD) of parabolic shaped cup. The 2-D interval halving method was found to be well suited for feasible region search in a large search space such as the metal forming parameters. The response surface method was used to construct a response surface of the process parameters in the feasible region and corresponding part quality. The constructed surface was then used to determine the optimal point using the simplex optimization method. Based on the finite element simulation results for hydromechanical deep drawing of the parabolic cup, the optimal blank holder force and maximum pressure of the quarter model were determined to be 63,125 N and 27.625 MPa, which resulted in a good part with only 33.21% thinning just 16 simulations.

This FEA based optimization approach developed and implemented in this work is believed to reduce lead time and effort spent in the HMD process parameter design significantly. Nevertheless, these predicted process parameters obtained need testing in real HMD experiments in the near future work, as to validate and improve the developed optimization approach.

## **ACKNOWLEDGEMENT**

The authors are pleased to acknowledge the National Metal and Materials Technology Center for using the LS-Dyna software.

## REFERENCES

- [1] S. H. Zhang, L. H. Lang, D. C. Kang, J. Danckert, and K. B. Nielsen, "Hydromechanical deep-drawing of aluminum parabolic workpieces-experiments and numerical simulation," *International Journal of Machine Tools and Manufacture*, vol. 40, no. 10, pp. 1479-1492, 2000.
- [2] S. H. Zhang, K. B. Nielsen, J. Danckert, D. C. Kang, and L. H. Lang, "Finite element analysis of the hydromechanical deep-drawing process of tapered rectangular boxes." *Journal of Materials Processing Technology*, vol. 102, no. 1-3, pp. 1-8, 2000.
- [3] S. H. Zhang, M. R. Jensen, K. B. Nielsen, J. Danckert, L. H. Lang, and D. C. Kang, "Effect of anisotropy and prebulging on hydromechanical deep drawing of mild steel cups," *Journal of Materials Processing Technology*, vol. 142, no. 2, pp. 544-550, 2003.
- [4] L. Lang, J. Danckert, and K. B. Nielsen, "Investigation into the effect of pre-bulging during hydromechanical deep drawing with uniform pressure onto the blank," *International Journal of Machine Tools and Manufacture*, vol. 44, no. 6, pp. 649-657, 2004.
- [5] L. Lang, J. Danckert, K. B. Nielsen, and X. Zhou, "Investigation into the forming of a complex cup locally constrained by a round die based on an innovative hydromechanical deep drawing method," *Journal of Materials Processing Technology*, vol. 167, no. 2-3, pp. 191-200, 2005.
- [6] W. J. Roux, N. Stander, and R. T. Haftka, "Response surface approximations for structural optimization," *International Journal for Numerical Methods in Engineering*, vol. 42, no. 3, pp. 517-534, 1998.
- [7] M. Kleiber, J. Rojek, and R. Stocki, "Reliability assessment for sheet metal forming operations," *Computer Methods in Applied Mechanics and Engineering*, vol. 191, no. 39-40, pp. 4511-4532, 2002.
- [8] L. Wang and T. C. Lee, "Controlled strain path forming process with space variant blank holder force using RSM method," *Journal of Materials Processing Technology*, vol. 167, no. 2-3, pp. 447-455, 2005.
- [9] K.-J. Lee, S. Kumai, T. Arai, and T. Aizawa, "Interfacial microstructure and strength of steel/aluminum alloy lap joint fabricated by magnetic pressure seam welding," *Materials Science and Engineering: A*, vol. 471, no. 1-2, pp. 95-101, 2007.
- [10] T. Khandeparkar and M. Liewald, "Hydromechanical deep drawing of cups with stepped geometries," *Journal of Materials Processing Technology*, vol. 202, no. 1-3, pp. 246-254, 2008.
- [11] E. J. Obermeyer and S. A. Majlessi, "A review of recent advances in the application of blank-holder force towards improving the forming limits of sheet metal parts," *Journal of Materials Processing Technology*, vol. 75, no. 1, pp. 222-234, 1998.
- [12] W. Thomas, "Product tool and process design methodology for deep drawing and stamping of sheet metal parts," Ph.D. Dissertation, Ohio State University, Ohio, 1999.
- [13] A. Haddad, R. Arrieux, and P. Vacher, "Use of two behaviour laws for the determination of the forming-limit stress diagram of a thin steel sheet: results and comparisons," *Journal of Materials Processing Technology*, vol. 106, no.1-3, pp. 49-53, 2000.
- [14] M. G. Cockcroft and D. J. Latham, "Ductility and workability of metals," *Journal of the Institute of Metals*, vol. 96, pp. 33-39, 1968.
- [15] Z. Q. Sheng, S. Jirathearanat, and T. Altan, "Adaptive FEM simulation for prediction of variable blank holder force in conical cup drawing," *International Journal of Machine Tools and Manufacture*, vol. 44, no. 5, pp. 487-494, 2004.
- [16] M. Zampaloni, N. Abedrabbo, and F. Pourboghrat, "Experimental and numerical study of stamp hydroforming of sheet metals." *International Journal of Mechanical Sciences*, vol. 45, no. 11, pp. 1815-1848, 2003.
- [17] M. Koç, *Hydroforming for Advanced Manufacturing*. Edited by Muammer Koç. New York: Woodhead Publishing Limited and CRC Press LLC, 2008.
- [18] Y. Huang, Z. Y. Lo, and R. Du, "Minimization of the thickness variation in multi-step sheet metal stamping," *Journal of Materials Processing Technology*, vol. 177, no. 1-3, pp. 84-86, 2006.